

A low cycle fatigue model for low carbon manganese steel including the effect of dynamic strain aging

Zhi Yong Huang^{a,*}, Danièle Wagner^b, Qing Yuan Wang^a, Muhammad Kashif Khan^a, Jean-Louis Chaboche^c

^a Sichuan University, School of Aeronautics and Astronautics, No.29 Jiuyanqiao Wangjiang Road, Chengdu 610064, China

^b Université Paris Ouest Nanterre La Défense, France

^c ONERA, DMSM, 29 avenue de la Division Lecerc, F-92320, Chatillon, France

ARTICLE INFO

Article history:

Received 29 September 2015

Received in revised form

9 December 2015

Accepted 11 December 2015

Available online 14 December 2015

Keywords:

Carbon manganese steel

Cyclic hardening

Dynamic strain aging

Low cycle fatigue

ABSTRACT

Carbon–manganese steel A48 (French standards) is used in steam generator pipes of the nuclear power plant where it is subjected to the cyclic thermal load. The Dynamic Strain Aging (DSA) influences the mechanical behavior of the steel in low cycle fatigue (LCF) at favorable temperature and strain rate. The peak stress of A48 steel experiences hardening–softening–hardening (HSH) evolution at 200 °C and 0.4% s^{−1} strain rate in fatigue loading. In this study, isotropic and kinematic hardening rules with DSA effect have been modified. The HSH evolution of cyclic stress associated with cumulative plastic deformation has also been estimated.

© 2015 Elsevier B.V. All rights reserved.

1. Introduction

Low Cycle Fatigue (LCF) loading produce damage in the service life of steam generator feed water lines of the Pressurized Water Reactor (PWR) [1,2]. The insufficient killed steel A48 used in these reactors is sensitive to the loading with different strain rates. Due to this, the metallurgical instabilities like Lüders bands, Portevin–le Chatelier bands [3–5] and DSA under tensile and fatigue loading are common in the alloy. DSA appears due to the interaction of strong solute atoms pinning and dislocations. The solute atoms are capable of diffusing over the short distance and arrest mobile dislocations at specific strain rate and temperature range. The strain rate sensitivity coefficient becomes negative due to DSA which helps in development of localized deformation bands (Portevin – Le Chatelier) in the monotonic tensile loading [5]. In low cycle fatigue, double cyclic hardening is observed in the peak tensile stress evolution [6].

Though multi-scale approaches have made great progress in the past 20 years, the existing macroscopical model of the constitutive framework is still widely used in the structure simulation and needs further improvement at continuum scale. The use of the yield surface in macroscopic cyclic plasticity theories ensures the accurate description of the Bauschinger effect. The Armstrong and

Frederick (A–F) [7] model, improved by Chaboche [8], Cailletaud [9], Macdowell [10], Ohno [11], Kang [12] and Khan [13] is suitable for the description of cyclic kinematic hardening. The splitting of the back stress into several parts was found to be successful for kinematic hardening in the LCF. The memory surface was introduced to well estimate the strain amplitude and loading sequences effects for the cyclic plasticity [14–15]. Recently, the cyclic viscoplastic modeling of the combustion chamber of aircraft engine material was investigated with DSA effect at elevated temperature [16].

This article focuses on the DSA effect on the LCF kinematic and isotropic hardening for the low carbon manganese steel. An improved constitutive model with DSA effects is proposed based on the thermodynamic framework and dislocation theory. The strain rate dependent rules of kinematic and isotropic hardening consider the interaction of the interstitial atoms with the gliding dislocations for stress – strain hysteretic response. The experimental results have been validated by implicit numerical integration method.

2. Material and testing

A48 steel is a kind of low carbon manganese steel (AFNOR NFA 36205 French Standard) which is used in the feed water line of French nuclear power plants [17]. A 40 mm thick plate undergoes a prior normalization and austenitising heat treatment at 870 °C

* Corresponding author.

E-mail address: huangzy@scu.edu.cn (Z.Y. Huang).

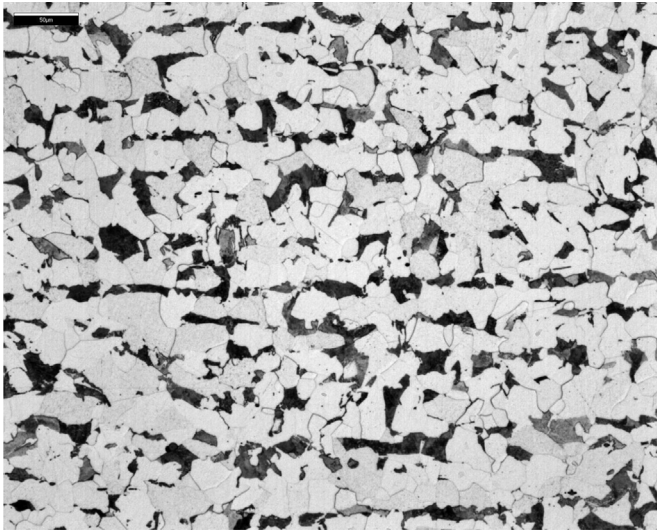


Fig. 1. Microstructure of A48 steel.

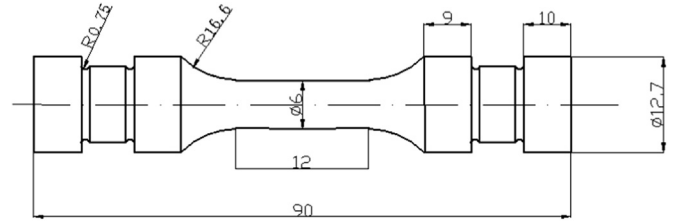


Fig. 2. Schematic illustration of low cycle fatigue specimen.

followed by air cooling. This forms a banded ferrite and pearlite grain distribution in the microstructure (Fig.1). Table 1 shows the chemical composition in weight percentage for the steel.

Low cycle fatigue specimen was designed as shown in Fig. 2. Low cycle fatigue tests were conducted under strain control mode in the hydraulic fatigue test machine (Instron 8501) at 0.4, 0.6 and 0.8% strain amplitude at 200 °C and 0.4% s⁻¹ strain rate.

The peak tensile stress curves are shown in Fig.3 at the strain amplitudes of 0.4, 0.6 and 0.8% at 200 °C. The cyclic stress response was dependent on the testing temperature and strain rate as shown in Fig. 4. It can be seen that there was an initial cyclic hardening after several loading cycles. This followed by a weak softening resulting in a secondary hardening at 200 °C in Fig.3.

Fig. 5 shows the LCF hysteresis loops for A48 at a strain rate of 0.4% s⁻¹ and 0.8% strain amplitude and 200 °C. The cyclic yield stress was obtained by the LCF test data (Fig. 5). It was found that the increase in cumulative plastic deformation change the stress-strain hysteretic response. The tangent slopes of the stress-strain hysteresis loops at the strain amplitude have been measured from the experimental data and shown in Figs. 6 and 7. The slopes grow significantly with increase in the number of cycles. However, the cyclic yield stress remained stable and showed the similar HSH behavior as shown in Fig. 8. This will be further discussed later in the article.

3. Modeling

3.1. Thermodynamic framework

In LCF, the plastic deformation forms hysteresis loop at the macroscopic scale. The thermodynamic potential (ψ) and the dissipation potential (ϕ^*) functions are given by:

$$\psi = \psi(\epsilon^e, T, \alpha_i) \tag{1}$$

$$\phi^* = \phi^*(\sigma, A_j, \epsilon^e, T, a_j) \tag{2}$$

Table 1
Chemical composition (wt%).

C	S	P	Si	Mn	Ni	Cr	Mo	Cu	Sn	Al	N	O
0.140	0.0057	0.016	0.225	0.989	0.024	0.021	0.002	0.027	0.003	0.045	0.0082	0.0006

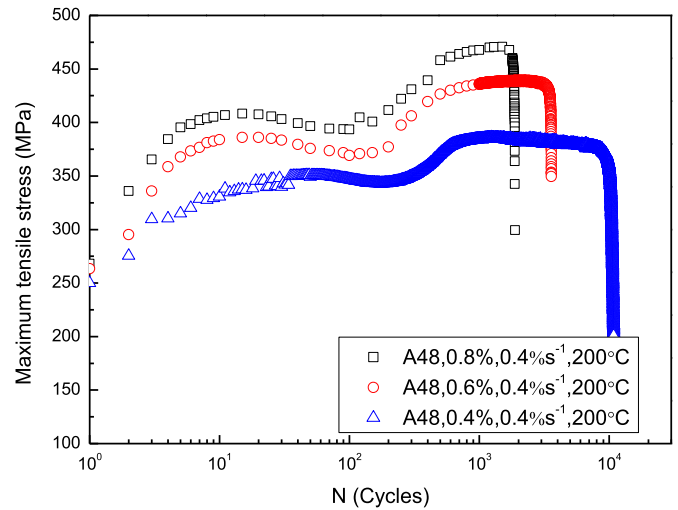


Fig. 3. Peak stress evolutions of A48 at 0.8%, 0.6% and 0.4% strain amplitudes in LCF with 0.4% s⁻¹ strain rate at 200 °C.

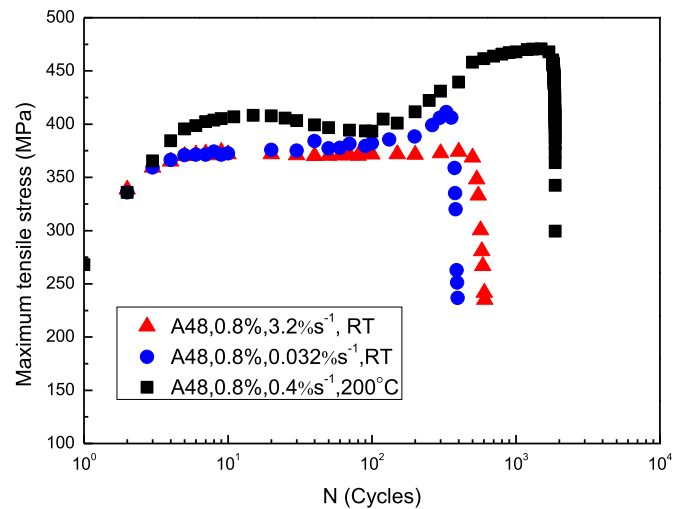


Fig. 4. A48 stress amplitude evolutions for $\epsilon_a = 0.8\%$ at room temperature at different strain rates.

ψ, ϕ^* are the functions which are assumed as follows [8]:

$$\rho\psi = \frac{1}{2}D_e: \epsilon^e: \epsilon^e + \frac{1}{3}ha: \mathbf{a} + W(r, T) \tag{3}$$

Download English Version:

<https://daneshyari.com/en/article/7975564>

Download Persian Version:

<https://daneshyari.com/article/7975564>

[Daneshyari.com](https://daneshyari.com)